We are IntechOpen, the world's leading publisher of Open Access books Built by scientists, for scientists

6,900
Open access books available

185,000
International authors and editors

200M
Downloads

Our authors are among the

154
Countries delivered to

TOP 1%
most cited scientists

12.2%
Contributors from top 500 universities

CLARIVATE ANALYTICS
BOOK CITATION INDEX
INDEXED

WEB OF SCIENCE™

Selection of our books indexed in the Book Citation Index
in Web of Science™ Core Collection (BKCI)

Interested in publishing with us?
Contact book.department@intechopen.com

Chapter

Integrated Electro-Optics Modulator

Yufeng Tao

Abstract

Electro-optic modulation (EOM) is an essentially important optical manipulation for on-chip photonics, optical communication and optical sensing. With emerging demands on efficient, broadband electro-optic modulation, the high-performance, integrated electro-optic modulation becomes indispensable. By manipulating phase or amplitude of optical field, optical information will be coded/modulated for communication or modulation. Through advanced micro/nano fabrication technique, the electro-optics crystal could be cut into the required volume/shape as specific, integrated modulator, waveguide or meta-surface for nano-photonic applications, paving a solid way for the imminent nano-photonic devices. Herein, the basic electro-optics effects, opto-electronic applications, methods of fabrication/integration, and future prospect of lithium niobate crystal are discussed or introduced. Demonstrations of box-sealed EOM, in-fiber EOM and the fabricated lithium niobate waveguides on substrate will be found here.

Keywords: electro-optics modulator, lithium niobate, micro/nano fabrication, nanometric interferometric sensing, on-chip photonics

1. Introduction

The emerging microwave photonics, optical communication network, photonic quantum computation and optical sensing require advanced electro-optics modulators with wide electrical modulation bandwidth (over 100 GHz), ultra-low optical insertion loss (<3 dB), scalable size, low half-wave drive voltage, ultra-fine signal quality, massively-producible fabrication ability and easy integration on various of insulator platforms [1–3]. Therefore, electro-optic modulators (EOMs) based on nonlinear optical materials such as lithium niobate ($LiNbO_3$), lithium tantalite ($LiTaO_3$), potassium titanium oxygenic phosphate ($KTiOP_4$), liquid crystal on silicon (LCOS) or 2D layered material modulator are often utilized to convert electronic signals to the optical domain via generating optical phase carrier or high-order harmonics, which are critical components in modern telecommunication networks and microwave-photonic systems [2, 4].

By inducing the known phase carrier via EOMs to specific optical field, the useful optical information will be coded/manipulated, and frequency character will be re-distributed, after receiving optical field by photodetectors or spectrometers, the delivered optical information could be reconstructed through algorithms [5–10]. In practical opto-electronic applications, the extensively-studied and applied $LiNbO_3$ often employs high driven voltage (>100 V) for relatively-low frequency band (DC to 1 GHz) in bulky size, while the resonant $LiNbO_3$ allows a radio-frequency slewing

rate (>1 GHz) at low driven voltages (<50 V, compatible to the CMOS devices). In addition of constant direct voltage, the external-applied electrical waveform could be sinusoidal, triangle, saw-tooth, trapezoid or other artificial waveforms.

Methods of self-growth of original bulky lithium niobate crystal is mature now, the real challenging mostly focuses on: (1) How to micro-miniaturize EOMs, massively-integrate them on various substrates [11–14]. (2) How to give large phase or amplitude variation in a tiny size EOMs, where short optical path inside EOM is helpful to decrease optical propagation loss [12, 15–17]. (3) How to improve their electro-optical efficiencies/group velocity matching/optical damage threshold [14, 17]. The solution of above challenges is highly-valued in optical communication networks/microwave photonics, quantum photonics and non-reciprocal optics [18].

Of great interest to broad application, the technological advance of micro/nanofabrication, high-power ultrafast laser processing makes the stiff, transparent crystal be artificially fabricated with ultrafine spatial resolution on substrate via high instantaneous power nanosecond or picosecond laser, which provides the key to integrate EOMs. Predictably, the imminent era of on-chip photonic devices via integrated EOMs will revolve optics, microwave, telecommunication, large-volume memory by providing tremendous new photonic applications.

2. Applications of lithium niobate

$LiNbO_3$ is a trigonal structure, wide transmittance range, non-linear optic crystal. Due to the spontaneous polarization, there exist electric dipole moments in lithium niobate crystals. The direction of these electric dipole moments tends to be consistent with the direction of outside-applied electric field, which affects the refractive index of the crystals. When being injected alternative or constant electric field, the resultant refractive index changes accordingly, making the optical phase shift as designed (seen in **Figure 1**), which is known as electro-optic effect. In optical communication or photonics, the optical signal passes through the lithium niobate crystal waveguide with alternating voltage, its equivalent optical path difference changes, inducing a controllable periodical phase shift or amplitude fluctuation [19].

Inside EOMs, the varying refractive index Δn presents a linear relationship with the applied electric field E:
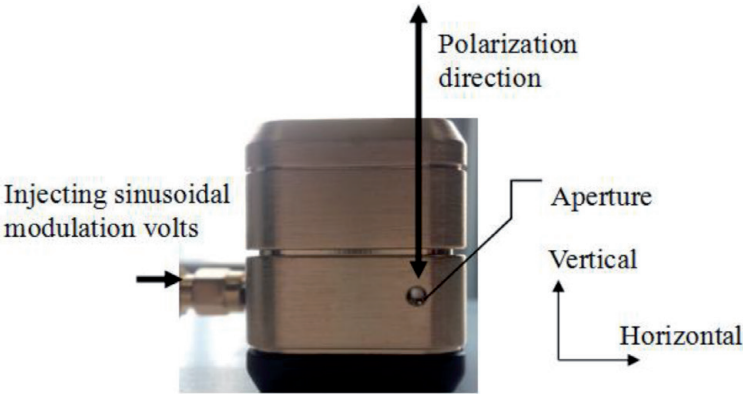
Figure 1.
A box-sealed, commercial magnesium oxide (MgO)-doped electro-optic modulator (4002, Newfocus), the crystal is installed with electronic drivers, diameter of aperture is <2 mm, allowing light to travel, phase-shifting happens only in the polarization direction.

$$\Delta n = \left(\frac{1}{2}n_e{}^3 r_{33}\right)E \tag{1}$$

Subsequently, the optical phase shifting replies on length and thickness of EOM and the outside-applied voltage V:

$$\phi_m = \frac{2\pi}{\lambda}\left(\frac{1}{2}n_e{}^3 r_{33}\right)\frac{d}{h}V \tag{2}$$

h is thickness, ϕ_m is the generated phase shift, n_e is dynamic refraction index of EOM injected with electric signal, λ is wavelength of light, r_{33} is the intrinsic nonlinear coefficient of EOM. The optical power damage threshold of MgO-doped EOMs (doping concentration: 5%) greatly increases, for general laser sources, the possibility of laser burning of electro-optic crystal becomes very small, which is beneficial to the long-term operation incorporating with high-power laser beam.

To get better electro-optic modulation efficiency, the polarization of laser and EOM should be paralleling. Otherwise, the dis-match will decrease the induced phase or amplitude shifting. It is noteworthy, the EOMs having intrinsic polarization could be furthered used in polarization-multiplexing optical system, which manipulate light at different polarization without optical cross-talk (**Figures 2** and **3**).

As simple demonstrated in **Figure 2**, the emitted laser beam is reflected by external vibrating target and injects into laser cavity, the reflected light affect by optical Doppler effect carries the information of external target to create a new fluctuated optical signal. When this optical signal travel in and out an EOM, the information is decoded artificially, which is a simple typical optical modulation application. By introducing polarization-multiplexing technique (where light has at least two polarizations), EOMs could modulate lights at different polarization for multi-channel communication, computation or sensing (as exampled by **Figure 3**) [9].

With technological advance, more situations (in-fiber optical communication) requires embedded in-fiber EOMs instead of spatially box-sealed EOMs, and highly-integrated photonic devices requires on-chip arrays of EOMs. Therefore, in order to minimize the weight and reduce the volume of LiNbO$_3$ for in-fiber embedded optical systems, LiNbO$_3$ wafer (or chip, widely fabricated via "ion slicing and direct bonding," seen in **Figure 4**) is optical lithographic patterned, cut and then annealing proton exchanged to form Y-type/S-type/line waveguide shapes. After polishing, the polished waveguide is aligned with polarization-maintaining fiber,
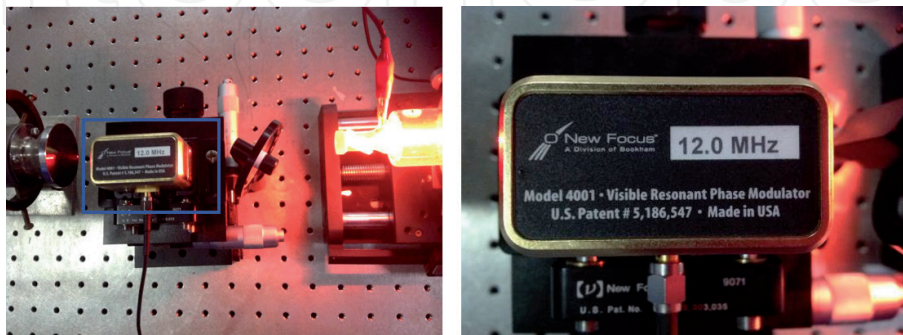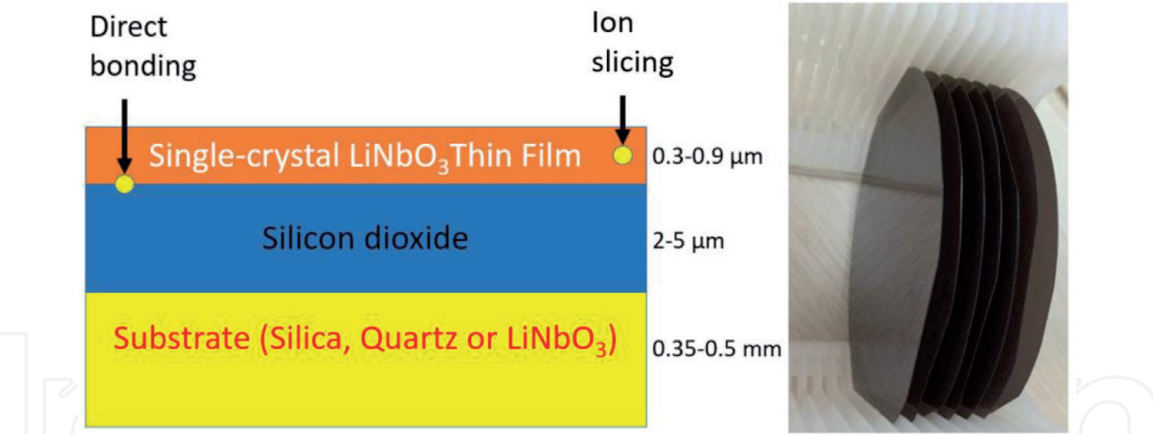

Figure 2.
A simple feedback laser system for recording sub-ultrasonic vibration of an ultrasound transducer. It consists of four main devices: a linearly polarized He-Ne laser (model: JW1, Beijing Topda laser), adjustable gradient optical density attenuator (model: NDC-50C-2M-A, Thorlabs), resonant phase modulator (model: 4001nf, Newfocus, 12 MHz central frequency, 36 V safe operating voltage, which is sealed with a resonant electric circuit) and an ultrasound transducer [10].
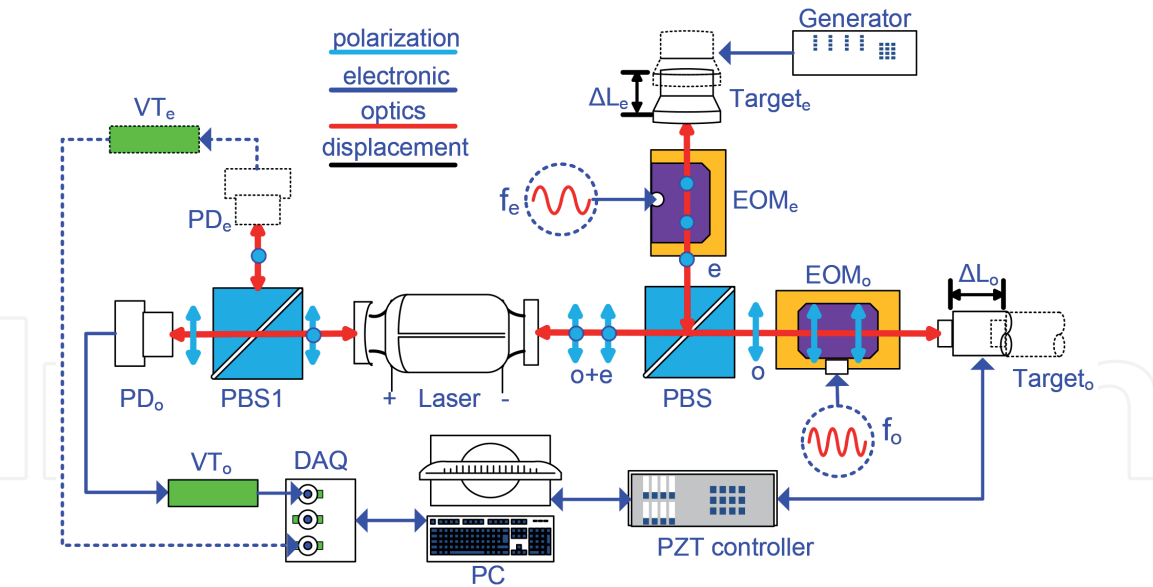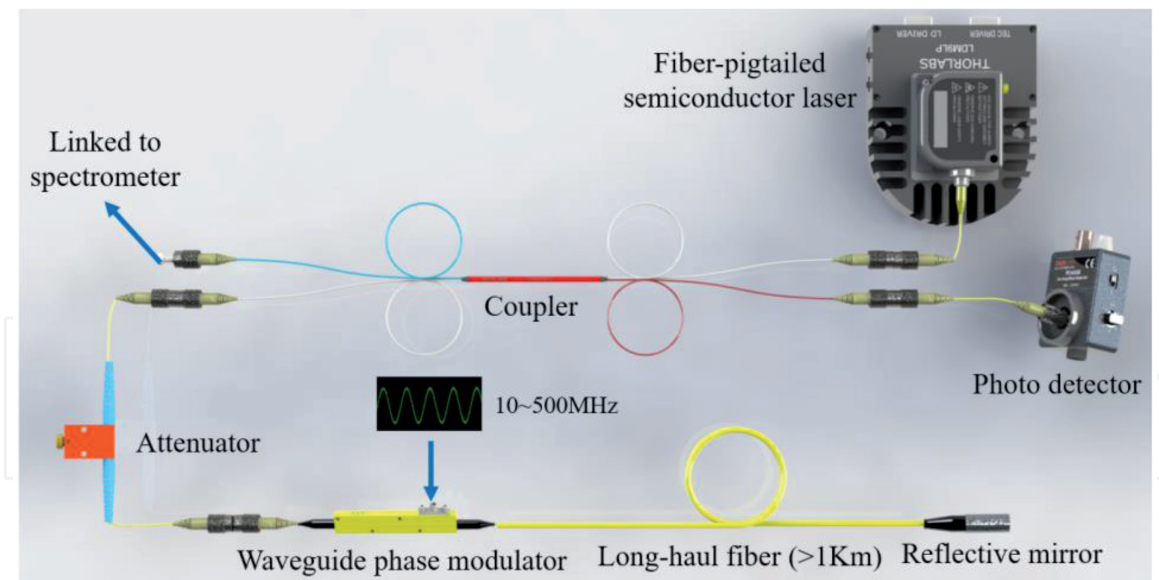
Figure 3.
A lensless two-dimensional polarization multiplexing phase-shifted self-mixing interferometry system is presented. The main devices include a two-longitudinal mode He-Ne laser, two electro-optic crystals with perpendicular polarizations, polarization splitter prism and two independent measured objects in different directions. Two linearly polarized lights are defined as o and e, VT represents adjustable resistance, computer (PC) takes responsibility of signal processing. The e-channel source is a speaker driven by AC voltage, and the o-channel source is a closed-loop one-dimensional piezoelectric ceramic (PZT). In this polarization-multiplexing system, the formed optical intensity fluctuations induced by the measured two external targets are modulated at different-frequency phase-shifting, therefore, no overlapping error happens after electro-optic modulation/manipulation [9, 10, 20].

Figure 4.
The standard "ion slicing and direct bonding" process for fabricating homogeneous or heterogeneous substrate-based thin $LiTaO_3$ or $LiNbO_3$ film, the right side are the fabricated $LiNbO_3$ wafers, which could be further X-cut or secondary etched for chip-scale electro-optic devices.

and then fixed in the shell. After connecting the lead wire of the electrode, the polished surface is packaged as in-fiber waveguide phase (or amplitude) modulator. Better than box-sealed EOMs, the integrated Y-shape waveguide phase modulator is easy to couple with in-fiber system and becomes bendable and suitable for fiber optical communication [13].

Y-shaped branch $LiNbO_3$ phase modulator contains three segments: input straight waveguide, symmetrical two S-shaped curved waveguide and two output straight waves. In the guide section, the input straight waveguide undertakes the tasks of connecting with the input optical fibers and equally distributing the power when the light enters the waveguide, and the two after the light comes back through the optical fiber. The minimum distance between two output waveguides must be

Figure 5.
A wave-guide phase modulator is inserted to the flexible, long-haul, in-fiber interferometric sensing system. Waveguide electro-optics modulator (Photoline, NIR-MPX800-LN-0.1, WPM) is driven by a low-voltage electronic signal (actually, using a microwave signal generator, the modulation frequency could be far beyond 500 MHz). The photo-electric detector (PD) with flange plate records the front output of semiconductor laser diode for further digital analysis, and an in-built photodetector inside semiconductor laser records the another optical intensity.

>0.25 mm when the diameter of polarization maintaining fiber (with cladding) is 0.25 mm. In the package process, polarization-maintaining fibers need to be bonded on small blocks before bonding with chips.

As demonstration of an in-fiber Y-shape phase modulator in laser beam manipulation, **Figure 5** illustrates a bendable optical configuration using in-fiber sealed waveguide type EOM, where fiber-pigtailed semiconductor laser (SL) is linked to a fiber-coupler, an optical power attenuator, and a 1 km-length standard single mode fiber (SMF). The Fabry-Perot SL (Thorlabs, LP852-SF30) emits an invisible 850 nm light, and possesses a sufficient sensitivity to the back-scattered weak light. A fraction of the emitted infrared light is back-scattered by an in-fiber mirror to re-enter into SL. To obtain optical phase variation, herein, the high slewing rate waveguide phase modulator (WPM) resonates from 10 to 500 MHz for phase shifting according to electric driven signal. Therefore, gauss beam of SL was transformed to a Bessel beam with over 10 M optical subdivisions.

Subsequently, logarithmic optical power loss of the 1180 m-length SMF (Yangtze, C5B00419AB2) by an optical power meter (PM100D, Thorlabs) is only 2.68 dB/km attenuation at 850 nm wavelength. The small power loss and high photon-current conversion efficiency of the SL guaranteed a long haul sensing. Semiconductor laser oscillation during the interferometric process depends on the reflected light and the phase shifting by the microwave-band WPM, which strictly follows the classical light-speed equation.

When the emitted and reflected optical fields couples together, and triggers laser frequency shifting $f \rightarrow f_0 + \Delta f$, the governing equation of dynamical oscillation condition changes to this form:

$$(g_0 + \rho \Delta N) f \frac{4\pi l}{c} = -\eta \cos\left(4\pi f \frac{\varphi}{c}\right) \tag{3}$$

$$(n_0 + \chi \Delta N) f \frac{4\pi l}{c} + \eta \sin\left(4\pi f \frac{\varphi}{c}\right) = 2\pi \tag{4}$$

where n_0 and g_0 denote initial values. χ and ρ are changing speeds of n and g to ΔN respectively. The delivered phase is affected by the external optical cavity length. The shifting optical frequency and fluctuating laser powers of front and rear facets are expressed as follows:

$$\Delta f = \frac{-\eta \sqrt{1+\alpha^2} \sin\left(4\pi f \varphi/c - \arctan(\alpha)\right)}{4\pi n_0 l \left(1 - \frac{g_0}{n_0}\alpha\right)} \tag{5}$$

$$\Delta P_{front/rear} = \mp m P_0 \cos\left(\varphi + \frac{1}{2}n_e^3 r_{33} E \sin\left(2\pi f_{RF} t\right) + \varphi_{speckle}\right) \tag{6}$$

where $\alpha = \frac{\chi}{\rho}$, E is the electrical field applied on the WPM. The Eq. (6) could be demodulated as Bessel functions using phase-resolved algorithm. Because the added
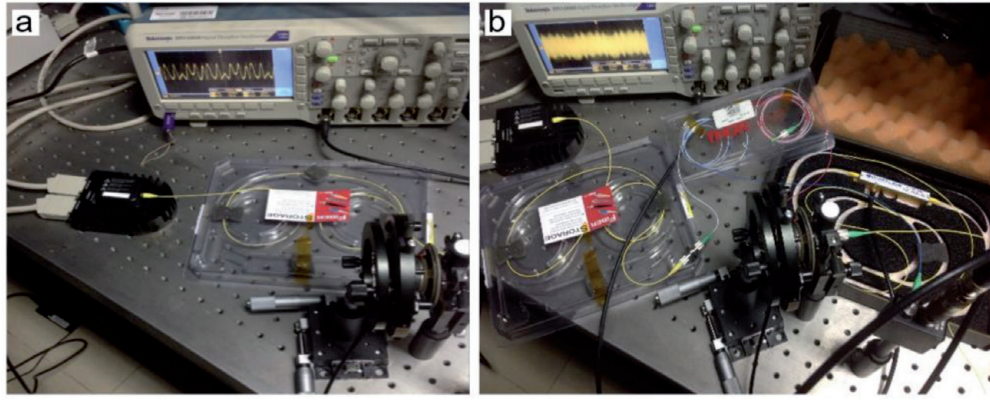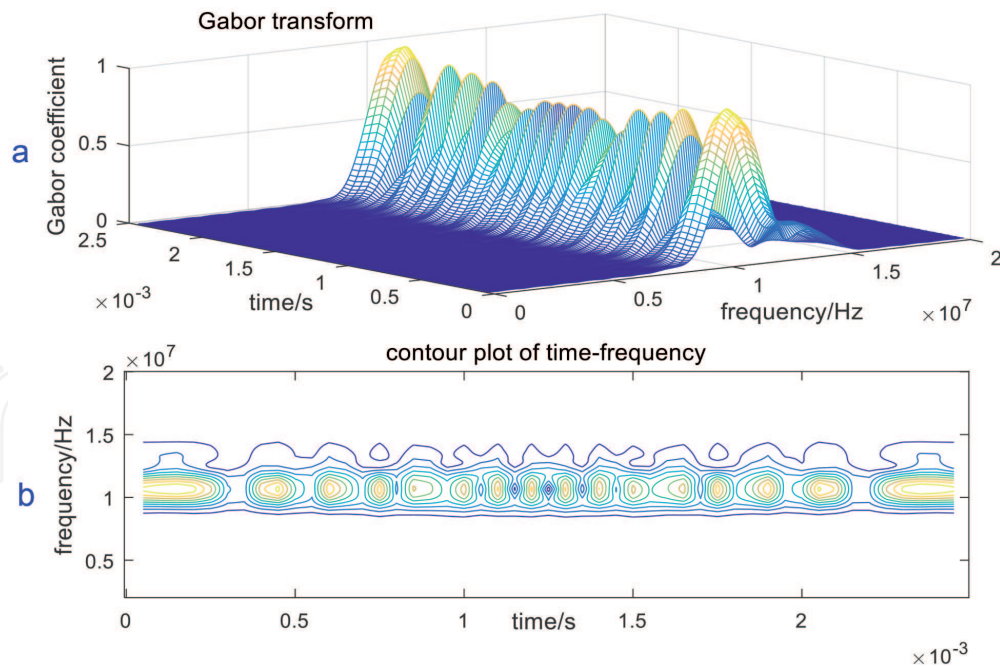

Figure 6.
Photos of in-fiber optical sensing experimental setup and observation of optical intensity fluctuation via oscilloscope. (a) Top view of vibration measurement without optical fiber phase modulator. (b) The view after inserting waveguide phase modulation is presented, including two-end input and two-end output optical fiber couplers, optical fiber waveguide phase modulator, loudspeakers as external reflector, the modulator is driven by a sinusoidal 17.5 MHz, 5 V electric voltage.
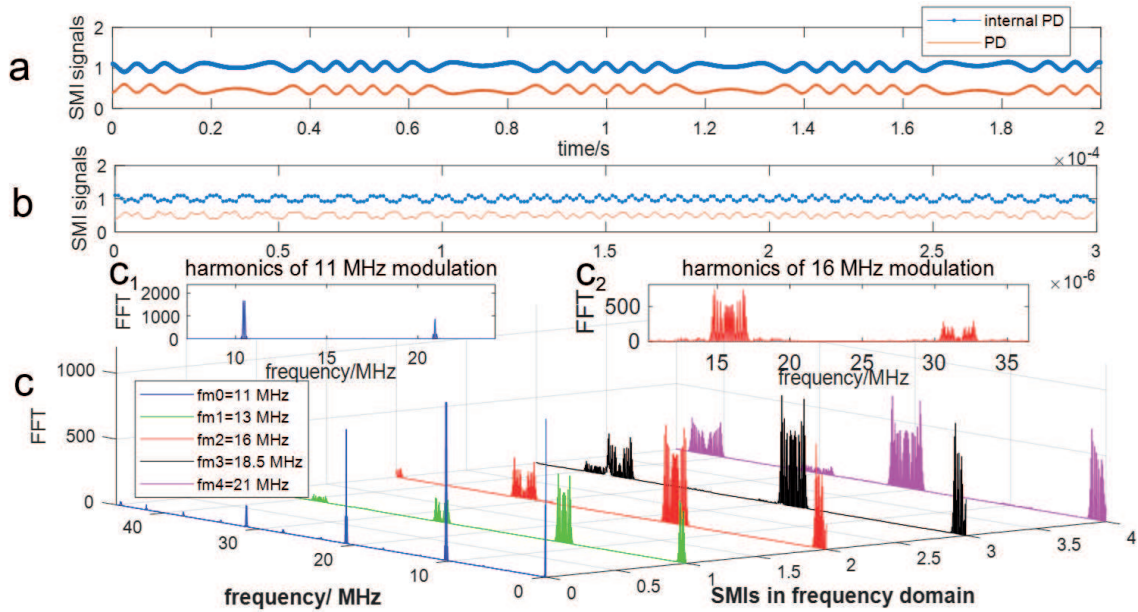
Figure 7.
Interferometric optical signals in time and frequency domains. (a) Synchronously-detected interferometric singles without activating electro-optics modulation (from PD and the photodetector of SL), presenting phase reversal phenomenon. (b) Interferometric signals of identical phase reversal when WPM slewed at 10 MHz/s. (c) Phase shifted interferometric signals in frequency domain. Zoomed-in figures C_1 and C_2 showed first-order and second-order harmonics, respectively.

Figure 8.
The first harmonic in joint time-frequency domain transformed by Gabor window when the modulation frequency was 11 MHz. (a) Three-dimensional distribution of Gabor coefficient of first harmonic of the phase-shifted optical field. (b) Time-to-frequency contour plot of (a), the center frequency fluctuates at around 11 MHz, known as the frequency of the applied electric field.

phase shifting is much faster than the target phase information, phase shifting induced by WPM operates as high-frequency phase carrier in subsequent decoding (**Figure 6**).

The frequency-domain signals of the electro-optic modulated intensity are obtained from fast Fourier transform (FFT) in **Figure 7**, where the optical harmonics concentrated around phase shifting frequencies with large adjoining space. Sufficient harmonic spaces eliminates the overlapping phenomenon for decoding accuracy. Gabor transform is implemented on the first harmonic of the phase shifted signals to show time-joint-frequency domain characteristics, which is similar to a straight mountain ridge (**Figure 8a**), concluding that the harmonic signal fluctuated around the phase shifting frequency.

3. Fabrication and integration

Currently, surface plasmonic polariton (SPP) devices have achieved desirable modulation of phase and amplitude, obtained by mesoscale fabrication technique. However, the metals that give plasmonic such promise are also the largest hindrance, as such devices suffer from large on-state loss. Still, typical insertion losses of 10 dB due to plasmonic propagation remains a concern for high-speed applications. Thus, plasmonic on-chip technologies have been unable to replace the existing electro-optics solutions [12, 15].

$LiNbO_3$-based devices, including in-fiber electro-optics modulators and other frequency converters, which are mostly fabricated via ion diffusion or proton exchange methods, leading to low index contrast and weak optical confinement. To address the future broad application of EOMs in chip-scale [16], the advanced micro/nanofabrication are often employed for sub-wavelength scale, massively-integrated $LiNbO_3$ platform to revolutionize optical communication and microwave photonics [17, 21, 22].

However, due to the hardness and stable chemical properties of $LiNbO_3$, traditional mechanical characterization or chemical etching methods can not achieve the micro/nano structures of lithium niobate with high spatial resolution. This problem
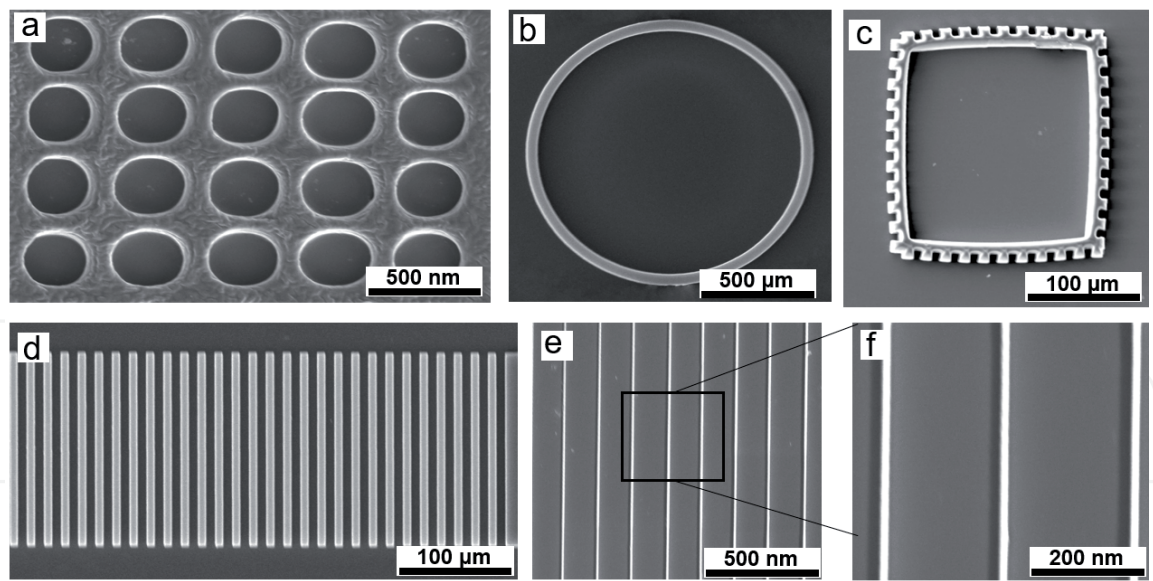
Figure 9.
Scanning electron microscope (SEM) images of (a) the hole array drilled by FIB on LiNbO$_3$ thin film. (b) (c) Ring-shape LiNbO$_3$ waveguide. (c) Square-shape waveguide. (d) Array of micro-wires of LiNbO$_3$ micro-wire circuit. (e) and (f) Zoomed-in SEM image of nanowires.
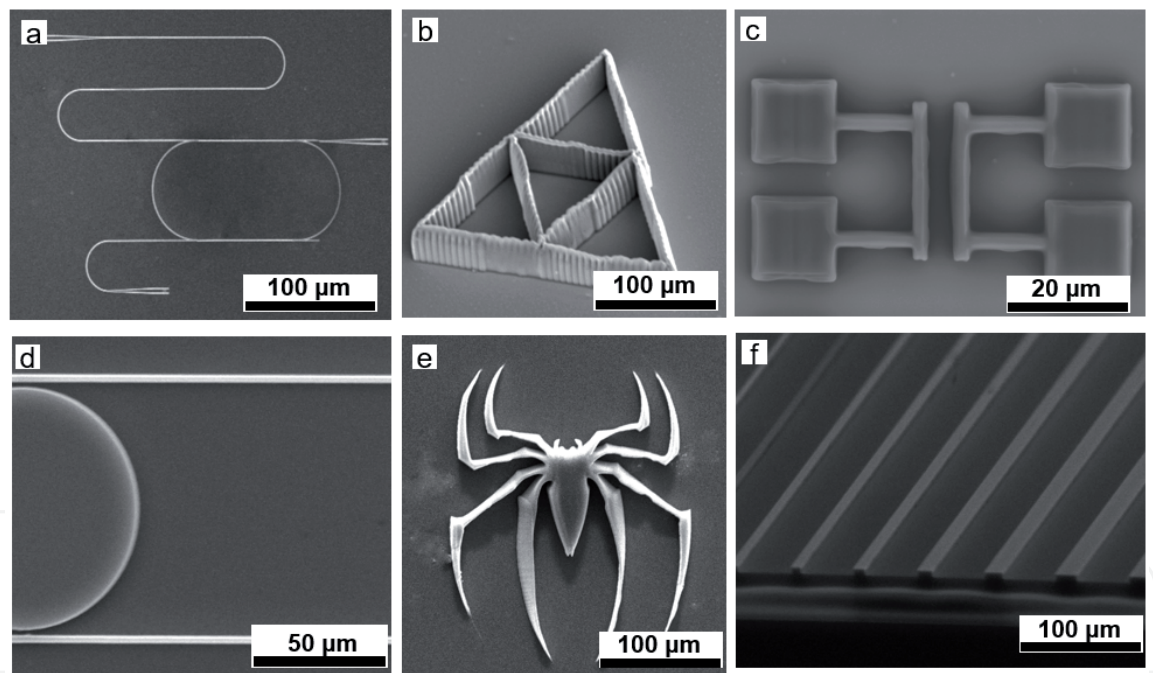
Figure 10.
(a–f) More fabricated photonic LiNbO$_3$ waveguides and patterns on silicon, which demonstrate ultra-fine and flexible features.

has greatly hindered the development of miniaturized and integrated lithium niobate photoelectric chips and devices. Major roadblock for the practical application of integrated LiNbO$_3$ photonics is the difficulty of fabricating devices that simultaneously achieve low optical propagation loss and high confinement.

Recently-developed thin-film LiNbO$_3$-on-insulator technology makes this possible. Several mainstream techniques like the acid etching, ion etching, plasma etching, optical lithography, high-power nanosecond or picosecond laser writing, electron beam writing or focused ion beam (FIB) etching are used to fabricate and integrate the tiny-size LiNbO$_3$ (nano-scale surface roughness and complicated arrangement, usually on micro-scale silicon dioxide or silicon substrates) waveguide

for device-level applications. The fabrication resolution of ultrafast laser cutting is typically in the order of 1 μm for glass, semiconductors and metals. However, today's optical lithography can easily achieve sub-micron resolutions [15, 18, 23, 24].

The standard electron beam lithography is firstly used to define patterns in photoresist, the patterns are subsequently transferred into the $LiNbO_3$ thin film using plasma reactive ion etching, the plasma power and chamber condition are artificially tuned to remove $LiNbO_3$ or contaminations, and after removing the photoresist, the pre-designed $LiNbO_3$ patterns in wafer/chips will be obtained. Or, by selectively bombarded and removed lithium niobate molecule via high-energy gallium ion beam, the arrays of nanowires, or nanowall-like $LiNbO_3$ devices could be obtained (seen in scanning electron microscope, SEM images, in **Figures 9** and **10**). Moreover, the nanofabrication technique could provide optical micro-resonators or photonic crystals. After furtherly interconnecting with driven electric circuits, on-chip integrated EOMs are expected to provide huge controllable photonic functions.

Photonic circuits based on $LiNbO_3$ waveguide have shown the potential for complex information processing systems employing both quantum and classical light sources [24]. To increase computational efficiency, new substrate materials (silicon, semiconductor materials, or fused silica) have been utilized to construct complicated resonant electro-optics modulators [18]. Silicon provides high refractive index enabling the fabrication of photonic circuits with strong confinement (seen in **Figure 10**). Specifically, silicon photonics maximize their modulation depth by using the resonant structures, enabling more compact components than in-fiber integration [17].

4. Conclusions

The electro-optics modulation capability of $LiNbO_3$, box-sealed packaging, applications of interferometric optical sensing via electro-optic manipulating light field are firstly demonstrated here. Then, the in-fiber integration of electro-optic modulation, and the existing micro/nano fabrications for on-chip $LiNbO_3$ waveguides are introduced. The background knowledge of $LiNbO_3$, advantages and inferiority of different kinds of sealing method and fabrication methods are presented as reminder for near-future broad applications of EOMs. We believe the integrated EOMs, is the future of the emerging on-chip microwave photonics, quantum optics and optical communication network. The ultralow loss, high optical confinement and the ability to connect to microwave electrodes will bring electro-optic and nonlinear optical systems to a micro/nano scale, massive application that has been inaccessible until now, which deserves a better and deeper investigation.

Acknowledgements

Conflict of interest

The author declare no conflict of interest in this chapter.

Author details

Yufeng Tao
Wuhan National Laboratory for Optoelectronics, Huazhong University of Science
and Technology, Wuhan, China

*Address all correspondence to: wsnwp520@sina.com

IntechOpen

References

[1] Oulton RF, Sorger VJ, Genov DA, Pile DFP, Zhang X. A hybrid plasmonic waveguide for subwavelength confinement and long-range propagation. Nature Photonics. 2008;**2**:496-500. DOI: 10.1038/nphoton.2008.131

[2] Gheorma IL, Osgood RM. Fundamental limitations of optical resonator based high-speed EO modulators. IEEE Photonics Technology Letters. 2002;**14**:795-797. DOI: 10.1109/lpt.2002.1003096

[3] Haffner C et al. Plasmonic organic hybrid modulators: Scaling highest speed photonics to the microscale. Proceedings of the IEEE. 2016;**104**:2362-2379. DOI: 10.1109/jproc.2016.2547990

[4] Sun ZP, Martinez A, Wang F. Optical modulators with 2D layered materials. Nature Photonics. 2016;**10**:227-238. DOI: 10.1038/nphoton.2016.15

[5] Alloatti L, Cheian D, Ram RJ. High-speed modulator with interleaved junctions in zero-change CMOS photonics. Applied Physics Letters. 2016;**108**:131101. DOI: 10.1063/1.4944999

[6] Maier SA et al. Plasmonics—A route to nanoscale optical devices. Advanced Materials. 2001;**13**:1501-1505. DOI: 10.1002/adma.200390134

[7] Vahala KJ. Optical microcavities. Nature. 2003;**424**:839-846. DOI: 10.29172/5802dce1007946889f4ea79871191efc

[8] Xu Q, Schmidt B, Pradhan S, Lipson M. Micrometre-scale silicon electro-optic modulator. Nature. 2005;**435**:325-327. DOI: 10.1038/nature03569

[9] Tao YF, Wang M, et al. Compound cavity theory of resonant phase modulation in laser self-mixing ultrasonic vibration measurement. Optical Engineering. 2016;**55**:074107. DOI: 10.1117/1.oe.55.7.074107

[10] Tao YF, Wang M, et al. Carrier-separating demodulation of phase shifting self-mixing interferometry. Optics and Laser Technology. 2017;**89**:75-85. DOI: 10.1016/j.optlastec.2016.08.013

[11] Poberaj G, Hu H, Sohler W, Günter P. Lithium niobate on insulator (LNOI) for micro-photonic devices. Laser & Photonics Reviews. 2012;**6**:488-503. DOI: 10.1002/lpor.201100035

[12] Wang C, Zhang M, Stern B, Lipson M, Lončar M. Nanophotonic lithium niobate electro-optic modulators. Optics Express. 2018;**26**:1547-1555. DOI: 10.1364/oe.26.001547

[13] Mercante AJ et al. 110 GHz CMOS compatible thin film $LiNbO_3$ modulator on silicon. Optics Express. 2016;**24**:15590-15595. DOI: 10.1364/oe.24.015590

[14] Jin S, Xu L, Zhang H, Li Y. $LiNbO_3$ thin-film modulators using silicon nitride surface ridge waveguides. IEEE Photonics Technology Letters. 2016;**28**:736-739. DOI: 10.1109/lpt.2015.2507136

[15] Haffner C et al. Low-loss plasmon-assisted electro-optic modulator. Nature. 2018;**556**:483-486. DOI: 10.1038/s41586-018-0031-4

[16] Sun C et al. Single-chip microprocessor that communicates directly using light. Nature. 2015;**528**:534-538. DOI: 10.1038/nature16454

[17] Reed GT, Mashanovich G, Gardes FY, Thomson DJ. Silicon optical modulators.

Nature Photonics. 2010;**4**:518-526. DOI: 10.1038/nphoton.2010.179

[18] Janner D, Tulli D, García-Granda M, Belmonte M, Pruneri V. Micro-structured integrated electro-optic LiNbO$_3$ modulators. Laser & Photonics Reviews. 2009;**3**:301-313. DOI: 10.1002/lpor.200810073

[19] Tao YF. Key technology of self-mixing micro/nano vibration measurement [thesis]. Nanjing Normal University; 2017

[20] Tao YF, Xia W, et al. Integration of polarization-multiplexing and phase-shifting in nanometric two dimensional self-mixing measurement. Optics Express. 2017;**25**:2285-2298. DOI: 10.1364/oe.25.002285

[21] Fortier TM et al. Generation of ultrastable microwaves via optical frequency division. Nature Photonics. 2011;**5**:425-429. DOI: 10.1038/nphoton.2011.121

[22] Tzuang LD, Fang K, Nussenzveig P, Fan S, Lipson M. Non-reciprocal phase shift induced by an effective magnetic flux for light. Nature Photonics. 2014;**8**:701-705. DOI: 10.1038/nphoton.2014.177

[23] Tao YF, Wei CYR, Liu JW, Deng CS, Cai S, Xiong W. Nanostructured electrically conductive hydrogels obtained via ultrafast laser processing and self-assembly. Nanoscale. 2019;**11**(18):9176-9184. DOI: 10.1039/C9NR01230C

[24] Wooten EL et al. A review of lithium niobate modulators for fiber-optic communications systems. IEEE Journal of Selected Topics in Quantum Electronics. 2000;**6**:69-82. DOI: 10.1109/2944.826874